# Effects of riverbank restoration on the removal of dissolved organic carbon by soil passage during floods - a scenario analysis

J. Derx[a,c,*], A. H. Farnleitner[d,b,c], G. Blöschl[a,b], J. Vierheilig[d,b,c], A.P. Blaschke[a,b,c]

[a] *Institute of Hydraulic Engineering and Water Resources Management, Vienna University of Technology, Karlsplatz 13, 1040 Vienna, Austria, phone: +43158801-22223, fax: +43158801-22399*
[b] *Centre for Water Resource Systems, Vienna University of Technology*
[c] *Interuniversity Cooperation Centre Water and Health, Vienna University of Technology*
[d] *Institute for Chemical Engineering, Research Area Applied Biochemistry and Gene Technology, Research Group Environmental Microbiology and Molecular Ecology, Vienna University of Technology, Vienna, Austria*

---

## Abstract

River restoration typically aims at improving and preserving the ecological integrity of rivers and their floodplains. Restoration projects may, however, decrease the ability of the riparian zone to remove contaminants as the river water moves into the aquifer, especially during high river discharges. The purpose of this paper is to analyze several factors involved during riverbank restoration (i.e. changes in riverbank topography and hydraulic conductivity of the upper sediments of the riverbank), with respect to their effect on enhancing dissolved organic carbon (DOC) transport from rivers into the groundwater. 3-D groundwater flow and transport with first-order decay was simulated for a typical setting of a porous groundwater aquifer near a large river. The simulations indicate that, during a 5 m flooding event, DOC concentrations in the groundwater can be 1.7 to 9 times higher at a restored riverbank (i.e. 250 m wide, no clogging within one meter of riverbank sediments) compared to a steep riverbank (i.e. 8 m wide, clogging within one meter of sediments), in coarse to fine sandy gravel. 51 to 89 % of this increase in DOC concentration levels in the groundwater were due to an increase in submerged area of the riverbank, depending on the type of soil of the aquifer. The remaining part was caused by a change in riverbank hydraulic conductivity. The simulations further showed that the arrival times of DOC concentration peaks at 400 to 500 m distance from the river axis can be 18 to 27 days shorter at restored than at steep riverbanks. 77 to 100 % of the earlier arrival times of DOC concentration peaks at 400 to 500 m from the river axis were due to an increase in submerged area of the riverbank. The remaining part was due to a change in riverbank hydraulic conductivity. The effects of riverbank restoration on DOC concentrations and arrival times were bigger if river DOC concentrations increased than if they were assumed constant during the flood, the more the river water level increased and the closer the distance was to the river. The findings suggest that riverbank restoration projects as conducted as part of the implementation of the European Water Framework Directive, potentially, may have adverse effects on the groundwater quality near rivers. Additional monitoring strategies will therefore be needed in the future in such projects to protect alluvial ground water resources for public drinking water supply.

*Keywords:* riverbank filtration, ecological integrity, water supply, DOC transport

---

## 1. Introduction

Aquifers are part of a valuable water resource system for drinking water supply. The water levels of rivers are affected by hydrological events (e.g. precipitation, snow melts) and by the regulation of rivers (e.g. power plants, etc.). The river water quality during floods may deteriorate e.g. due to combined sewer overflow events or direct runoff from areas with intensive agriculture (stock farming, Kirschner et al. 2009, etc.). Floods may cause strong variations in flow velocities near rivers and may significantly shorten the travel times of contaminants from the river to a drinking water well (Shankar et al. 2009). Moreover floods can cause that contaminants are transported further into groundwater (Derx et al. 2010, 2013a). In addition, bank sediments may be mobilized by lateral erosion leading to a temporary increase of river water infiltration (Regli 2007, Woolsey et al. 2007). Initiatives for restoring rivers typically have the aim to improve and preserve the ecological quality of rivers and their floodplains.

Restoration measures, such as the widening of the river bed, aim to increase the functional diversity which may improve the natural biological community of groundwater (Samaritani et al. 2011). Restoration measures moreover lead to changing bank morphologies and hydraulic conductivities of bank sediments, which generally increase the degree of river-groundwater interaction. Concerns have been raised that these measures may be detrimental for groundwater quality (Hoehn and Scholtis 2011). As a consequence, Swiss regulations already prohibit river revitalization near production wells (BUWAL 2004). Groundwater quality may deteriorate due to elevated fractions of infiltrated river water and reduced subsurface residence times after riverbank restoration. As hydrologic and hydrogeochemical conditions commonly differ before and after riverbank restoration, these effects are difficult to predict and to quantify (Hoehn and Scholtis 2011). Vogt et al. 2010 compared the propagation of electric conductivity diurnal signals in groundwater and found shorter travel times between the River Thur and a drinking water well at a restored site than at a channelized section, despite similar distance to the river and aquifer hydraulic conductivity. The effects on contaminant transport during riverbank filtration are yet unknown.

The removal during riverbank filtration of contaminants is of great concern, which emerge in the aquatic environment and in waste water because of their use for human and veterinary purposes (Maeng et al. 2011). Among the contaminants in waters, which are of growing concern for the safety of drinking water, are pharmaceutically active compounds, endocrine disrupting compounds and personal care products. However, elaborate and costly detection techniques are often required for detecting these compounds in water. DOC is therefore most often used as a sum parameter for organic matter, which often occurs together with contaminants originating from waste water effluents (Maeng et al. 2011, Weiss et al. 2003, Partinoudi and Collins 2007). High levels of DOC can deteriorate the taste in drinking water and may lead to disinfection byproducts during chlorination of raw water (Schmidt et al. 2003, Hülshoff et al. 2009). DOC can be removed by adsorption onto aquifer materials or by biodegradation (Maeng et al. 2011). During biodegradation microorganisms utilize DOC for growing and for gaining energy, thus reducing DOC concentrations in water (Ludwig et al. 1997). An essential part of DOC concentration is reduced within the first meter of the sediments at the river-sediment interface, where microorganisms may actively grow bacterial biofilms and thus often reduce the hydraulic conductivity (i.e. sediment clogging, Cunningham et al. 1991). From a statistical analysis of a data set from 33 riverbank filtration sites in various countries, Skark et al. (2006) identified the most important factors for DOC elimination during riverbank filtration as the initial DOC concentration in the river, the transmissivity (i.e. hydraulic conductivity and thickness) of the aquifer and the residence time in groundwater. While the importance of riverbank hydraulic conductivity on groundwater quality is already known (Cunningham et al. 1991, Skark et al. 2006), the effect of changing riverbank topographies after restoration was not yet analyzed, especially not during floods. Larger submerged areas of riverbanks after restoration can lead to an enhanced river-aquifer mixing and may thus enhance DOC transport from rivers into groundwater. As DOC concentrations in rivers can vary greatly during floods, the risk of groundwater contamination may be high.

The primary objective of this paper is therefore to quantitatively analyze the effects of topographical changes of the riverbank and changes of riverbank hydraulic conductivities after restoration on DOC concentrations in the near-river groundwater during floods. The effects of variable DOC concentrations at the river boundary during floods were separately analyzed, as they may add to the effect of riverbank restoration on DOC concentrations in the near-river groundwater.

The secondary objective is to analyze the effects of riverbank restoration on DOC travel times from the river into the groundwater aquifer. After riverbank restoration, topographical changes of the riverbank or changes in hydraulic conductivity of the upper sediments of the riverbank may cause DOC concentrations to be transported further into the groundwater and to arrive earlier at a given distance from the river. The risk of groundwater contamination near rivers may therefore increase as a result of restoration, requiring additional treatment for drinking water. Scenarios of a large river and an aquifer with simplified geometries were assumed, allowing us to study the above effects independently from each other. This is considered an important first step in order to understand the mechanisms of riverbank restoration affecting groundwater quality from a hydraulic perspective.

This paper complements previous studies on river-aquifer interaction for larger river settings (Derx et al. 2010, Derx et al. 2013a and 2013b). Derx et al. (2010), (2013a) analyzed the effect of river level fluctuations on solute and virus transport from the river into the aquifer. Derx et al. 2013b examined temperature effects on the exchange. In contrast, this paper examines the factors of riverbank restoration that may enhance DOC in the groundwater by comparing scenarios with and without restoration.

## 2. Methods

We adopted the groundwater flow and transport model used in Derx et al. 2013a and 2013b, extended for a restored riverbank. A three-dimensional groundwater flow and transport model (SUTRA 2.1, Voss and Provost 2008) was coupled to a 1D surface water model (HEC-RAS, U.S. Army Corps of Engineers 2008), fully accounting for transient-variably saturated flow conditions. The simulated surface water levels were used as input to the groundwater flow and transport model by defining the simulated heads as specified pressure boundary conditions in time and space over the entire river bed (Section 2.2). The groundwater flow model was validated on data from a field site at the Austrian Danube with transient flow conditions during several flooding events. It was demonstrated that the transient groundwater flow situation during flooding events could be reproduced, with mean biases always less than 7 cm (Derx et al. 2010). For a detailed description of the water flow model coupled with transient surface water - groundwater interaction, see Derx et al. (2010).

### *2.1. Description of the groundwater flow and transport model*

Derx et al. 2013a found that river-aquifer mixing and dispersion were important for enhancing virus transport into groundwater during river water level fluctuation. As dispersion is therefore likely to be important also for our simulations and may be smaller when considering less dimensions, we considered 3-D groundwater flow and transport. Moreover, the groundwater flow situation is 3-D because the propagating flood wave causes return flows during the receding flood. At this point in time (after 20 d), the near-river groundwater flow direction is not perpendicular to the river axis (Figure 1, right). The general form of the 3-D variably saturated groundwater flow equation as solved in SUTRA 2.1 is

$$(\Theta_w \rho s_{op} + \Theta \rho \frac{\partial \Theta_w}{\partial p}) \cdot \frac{\partial p}{\partial t} - \vec{\nabla}[\frac{\rho K(\Theta_w)}{\mu}(\vec{\nabla} p + \rho \vec{g})] = 0, \tag{1}$$

for explanation of symbols see Table 1. The numerical solution of this equation is processed by a first linear projection of the nodal heads and iterative processing for resolving nonlinearities. Then the linear system of equations is solved using an iterative sparse matrix equation solver.

For simulating DOC transport in groundwater Equation 2 was used, which is based on the 3-D variably saturated advection-dispersion equation with first-order decay ($\lambda$), as solved by SUTRA2.1 (Voss and Provost 2008).

$$\frac{\partial \Theta\Theta_w \rho C}{\partial t} + \vec{\nabla}(\Theta\Theta_w \rho \vec{v} C) - \vec{\nabla}(\Theta\Theta_w \rho D \vec{\nabla} C) = -\Theta\Theta_w \rho \lambda C, \tag{2}$$

for explanation of symbols see Table 1.

The hypothetical aquifer scenarios were assumed for a steep and for a restored riverbank, as shown in Figure 1. The gradually submerged area during an increase of river water level by 5 m was assumed to be 8 m wide at the steep riverbank (corresponding to a slope of 2:3 of the riverbank) and 250 m wide at the restored riverbank (Figure 1). The larger area at the restored riverbank originates from restored riverbanks often failing under the influence of gravity until they end up in a stable state (Shields 1996).

### *2.2. Conceptual model and boundary conditions*

The model comprises an area of 9 by 4.6 km, limited by a straight river stretch of 9 km length (Figure 1, right). The river is 150 m wide and is delimited by the river centre line and the riverbanks. The model dimensions were chosen large enough to avoid errors caused by boundary effects. For the simulations we assumed a large river which has an oxygen content close to saturation. This is important for choosing the degradation rates of DOC later in this section. The unconfined alluvial aquifer is 10 m deep consisting of either coarse gravel, fine gravel and fine sandy gravel porous media and is fully connected to the river or partially overlain by a clogging layer on top of the riverbank and bed. These conditions are often found at riverbank filtration sites underlaid by fluvial gravel aquifers (Hoehn 2002, Homonnay 2002, Weiss et al. 2005, Schubert 2006).

As the aim was to simulate infiltration conditions, the boundary conditions were assigned so that water level gradients were directed naturally from the river into groundwater (the pressure gradient was assumed 3 m/km, see Figure 1). A straight 9 km long river stretch was assumed to overlay the aquifer (Figure 1, the river is shaded in blue). Head boundary conditions prescribed in this zone were set at the top elements of the river bed and bank based on the water levels of a hydrodynamic, 1D surface water model (HEC-RAS, U.S. Army Corps of Engineers 2008). The vertical exchange rates across the river bed are thus controlled by the transient water levels specified at the river bed boundary and the vertical hydraulic conductivity of the uppermost cell of the aquifer below the river bed. The dynamics of river flow and their effect on groundwater flow were fully accounted for. The simulated river water level increased by 5 m at maximum. The simulated flooding event mimics a real river flooding event and lasts for 20 d, followed by 40 d of steady low flow conditions (Figure 2). As a simplified assumption, the progression of the river stage was assumed to follow a cosine function.

At all vertical boundaries except for the one along the river, we used the same, constant prescribed head boundary conditions as for the initial condition. We defined the vertical boundary along the river axis to be no-flow since we assumed parallel flow along the river axis. Likewise, the top layer in the land zone was set to no-flow, as we assumed no groundwater recharge from precipitation. The bottom model boundary was defined to be no-flow, representing an impermeable layer of clay and silt below the aquifer. The transition zone between the highest and lowest water mark alternated between submerged and dry during the simulations (Figure 1, left). The boundary conditions in this zone were set according to the model result of the previous time step for a given node. If the hydraulic pressure of the previous time step was positive, the head boundary condition was set to the local surface water level. If the hydraulic pressure was negative, the boundary conditions were set to no-flow since the soil was unsaturated (as in Derx et al. 2010).

### *2.3. Model discretisation*

The horizontal discretizations of the numerical elements vary between 1.5 m and 100 m (Figure 1). As the effects of riverbank restoration are strongly influenced by river-aquifer mixing and dispersion in the near-river groundwater (e.g. Derx et al. 2010), it was important to avoid additional numerical dispersion. Along the riverbanks and in the centre of the model (Figure 1, right), numerical cell sizes were therefore kept small (1.5 to 10 m). The DOC transport simulations were evaluated in the detailed section of the model. The upstream and downstream boundaries were sufficiently far from this middle section so that numerical errors induced by the coarser mesh could be excluded (Figure 1, right). The aquifer was discretized into 20 layers ranging from 10 to 35 cm in the upper soil zone and from 1.2 to 1.5 m in the fully saturated zone (Figure 1, top left). The small vertical discretisation in the upper soil zone was required in order to resolve the nonlinearities of the unsaturated flow equation. For including clogging of river beds and banks the same model set-up was used with the difference that the uppermost 3 layers were discretized using a fixed vertical cell size of 10 cm. This way, the correct simulation of a thin layer of very low conductivity on the uppermost 3 elements of the riverbed and bank was ensured. The model consists of approximately 850,000 elements in total.

### *2.4. Model parameterisation*

The simulations were performed with an initial surface water depth of 0.5 m and 3 m (for river water levels increasing by 3-5 m and for steady flow, respectively). For the initial pressure conditions, simulations were performed with all boundary conditions held constant over a time long enough (1.5 years) so that the initial conditions had no influence on the groundwater flow results. For the transport simulations, an initial DOC concentration of 1 mg/l was assumed homogeneously distributed in groundwater, which was the average value observed in production wells nearby a number of large rivers (e.g. near the rivers Danube, Wolfram and Humpesch 2003, Orlikowski and Hein 2006, Missouri, Ohio and Wabash, Weiss et al. 2003, Soucook, Partinoudi and Collins 2007, Rhine, Schmidt et al. 2003 and Thur, Hoehn and Scholtis 2011). The DOC concentration of the river water during steady flow conditions was set to 3 mg/l, which is within the range of observed values in these and other middle European rivers (Skark et al. 2006). The DOC concentrations during an increase in river water levels by 3 and 5 m were either assumed as for the steady flow conditions or were assumed to increase from 1 mg/l to 5 mgl/s and 10 mg/l during a 3 and 5 m flood event, respectively (Figure 2, as observed e.g. in the Danube River by Wolfram and Humpesch 2003). The DOC concentrations were assumed homogeneously distributed in the river.

As the hydraulic conductivity in fluvial gravel aquifers near rivers often ranges from $10^{-3}$ m/s to $10^{-2}$ m/s (e.g. at the River Rhine, Schubert 2006 and Shankar et al. 2009, or other rivers, Skark et al. 2006), this range was assumed in our simulations. Out of this range, the maximum ($10^{-2}$ m/s), average ($5 \cdot 10^{-3}$ m/s) and minimum values ($10^{-3}$ m/s) of $K_f$ were assigned to coarse gravel, fine gravel and fine sandy gravel material. Each of these values was distributed homogeneously over the entire aquifer with an anisotropy ratio of 1:10, assuming effective parameters. The adopted aquifer was fully connected to the river or overlain by a clogging layer. This layer was assumed to have a thickness of 30 cm and a hydraulic conductivity of $10^{-6}$ $m/s$ on top of the river bed and on top of the steep riverbank (Grünheid et al. 2005, Blaschke et al. 2003, Fischer et al. 2005). Clogging processes may consist of several clogging cycles of a few weeks each initiated by floods until a stable state is reached (Blaschke et al. 2003). Rating curves often show a clear trend that suspended load concentrations in rivers are low during low river flows (Hickin 1995). Clogging will therefore typically establish slowly and during long time periods. During the 60 d of simulation time, the clogging layers were therefore assumed to remain constant.

For the effective porosity a range of 0.1-0.2 was reported for sandy gravel and gravel (de Marsily 1986). Assuming a worst case, we assigned the lowest value of 0.1 to the effective porosity. Water saturation and hydraulic conductivity in the unsaturated zone were calculated by using the model of van Genuchten 1980. The parameters $\alpha$, n and the residual water saturation $\Theta_r$ were set to 0.36 $kPa1$, 3.18 and 0.14, as obtained by the Rosetta Lite program (Schaap et al. 2001) for the sand textural class of the USDA triangle (Derx et al. 2013a and 2013b). The longitudinal and transversal dispersivity for the horizontal directions ($\alpha_l$) was set to 5 m and 1 m, respectively, in the detailed section of the model (Figure 1, right). The condition of Kinzelbach (1987) for the three-dimensional case and for small ratios of $\alpha_l$ / $\alpha_t$ ($<$ 10), as in our simulations, is thus fulfilled: $P_e$=v$\cdot\Delta$d/D $\leq$ 2, where $P_e$ is the Peclet number, D is the dispersion coefficient, $\Delta$d is the element size and v is the pore-water velocity. According to the ratio of horizontal to vertical element sizes, an anisotropy ratio of dispersivities of 0.1 was assumed. Separate simulations, where we compared anisotropy ratios of 0.1 and 0.01, showed that they were not important in our simulations (results not shown). Likewise for hydraulic conductivity, an anisotropy ratio of 0.1 was assumed (Chen 2000).

For simulating DOC transport, we assumed a contaminant undergoing slow irreversible sorption or first-order decay. Reversible sorption processes were assumed negligible in our simulations. As DOC decay depends on various parameters, such as the redox conditions in the aquifer, pH, temperature, etc., the decay rate is often estimated from a global mass balance of a DOC concentration plume in the field or in the laboratory (Rausch et al. 2005). From such global measurements of DOC decay in gravel aquifers near the Rhine (Schmidt et al. 2003), the Elbe (Fischer et al. 2005) and in a 30 m large column experiment (Grünheid and Jekel 2005), half-life values ($t_{1/2}$) from 30 to 50 d were observed. These half-life values are transformable into decay rates from 0.01 to 0.02 $d^{-1}$, given the relation $\lambda = ln2 / t_{1/2}$ (Rausch et al. 2005). Alternatively, DOC decay rates were determined in gravelly porous media from the exponential decline in observed breakthrough curves during field experiments (Schönheinz and Grischek 2011). The DOC decay rates reviewed by Schönheinz and Grischek (2011) for aerobic aquifer conditions ranged from 0.01 to 0.07 $d^{-1}$ (Krüger et al. 1998, Boggs et al. 1993). This range was therefore assumed for our scenarios. The largest decay rate value of $\lambda$=0.07 $d^{-1}$ was assigned to the finest type of porous medium because of a higher affinity to attach to sediments. For gravel and fine gravel material, $\lambda$=0.01 and 0.02 $d^{-1}$ were assumed, constant in each simulation run, even though the field experiments used for deriving $\lambda$ involved physical and chemical heterogeneities of the aquifer from a scale of 10 to 100 m.

## 3. Results

In the simulations during steady flow conditions there was a natural groundwater gradient from the river into the aquifer. During rising river water levels (from days 0-10), groundwater gradients near the river increased, thus more water entered the riverbank and DOC concentrations in the near-river aquifer increased (Figure 3). During falling river water levels (from days 10-20), the natural groundwater gradient turned from infiltration to groundwater exfiltration conditions (Figures 3 and 6, c and d, right). The simulated DOC concentrations responded on the return flows with a delay of 10 d. The DOC concentrations in Figures 3 and 6, c and d are therefore shown after 30 d of simulation time, while the groundwater flow directions are shown after 20 d of simulation time. These return flows into the river led to a significant decrease in DOC concentrations in groundwater at distances from 400 to 500 m from the river axis, following the peak of the flood after 10 d (Figure 7). The DOC concentrations over time from Figures 7 to 9 refer to the lowest depths of the aquifer because this is where the pipes of horizontal wells are usually located. In the simulations where DOC concentrations in the river increased concurrently during the floods and where clogging of the top sediments was assumed, the return flows only led to a decrease in DOC concentrations at the restored riverbank (Figures 3 and 6). At the steep riverbank, the DOC concentration peaks arrived with a delay of several days at distances from 400 to 500 m from the river axis, and therefore missed the time when the return flows occurred (after 10 to 20 d of simulation time).

### *3.1. Effect of aquifer material*

Simulated DOC concentrations in fine gravel were reduced from 10, 5 and 3 mg/l at 200 m from the river axis to 4.5, 2.5 and 1.8 mg/l at 500 m from the river axis (Figure 5, top centre). This is consistent with a relatively constant DOC concentration reduction of 50 % found at the Elbe River in Dresden, from 6.9 and 5.6 mg/l in the river to 3.4 and 3.2 mg/l near the production site 300 m from the river during measurements conducted in 1991/1992 and 2003, respectively (Fischer et al. 2005). The conditions at the Elbe River are very similar to the conditions assumed in our simulations, i.e. with an aquifer thickness of 15 m and a hydraulic conductivity of 0.6 to $2 \cdot 10^{-3}$ m/s.

The simulations in this paper showed that a larger area of the restored riverbank which is gradually submerged during a flood can cause higher DOC concentration levels in groundwater. Simulated DOC concentrations at the bottom of the aquifer were 1.1 times higher at the restored than the steep riverbank in coarse gravel, 1.3 times higher in fine gravel and 2.5 times higher in fine gravel with sand (0.3, 0.7 and 1.5 mg/l, respectively, Figure 4). When assuming that DOC concentrations in the river additionally varied from 1 to 10 mg/l during the flood, simulated DOC concentration levels at the bottom of the aquifer were 1.25 times higher in coarse gravel, 2 times higher in fine gravel and 9 times higher in fine gravel with sand at the restored than at the steep riverbank (2, 5 and 9 mg/l, respectively, Figure 5, top).

### *3.2. Effect of a clogging layer*

Figure 5, bottom shows that for the scenario of a steep riverbank a clogging layer led to more DOC removal in the first meter of the riverbank and bed sediments. This is consistent with reports of the most efficient removal in the oxic infiltration zone (Hülshoff et al. 2009). While for the steep riverbank scenario DOC entered the aquifer preferably below the river bed, DOC entered the aquifer preferably below the riverbank at the restored site (see black arrows in Figure 6, a and b). In the simulations for the restored riverbank, DOC concentrations were consequently not affected by clogging in the near-river groundwater, but were reduced more efficiently further from the river. The additional removal of a low hydraulic conductivity layer on top of the riverbank sediments after restoration caused that simulated DOC concentration levels at the bottom of the aquifer were 1.7 times higher in coarse gravel, 2 times higher in fine gravel and 9 times higher in fine gravel with sand than at the steep riverbank (4, 6 and 9 mg/l, respectively, Figure 5, bottom). If the river water level was assumed constant during the simulations ($\Delta h = 0$), sediment clogging had very little effect on DOC concentrations (Figure 5, bottom).

### *3.3. DOC time arrival*

Our simulations further showed that larger areas of the restored riverbank which are gradually submerged during the flood can cause that DOC concentration peaks arrive earlier at 500 m distance from the river axis in groundwater. Simulated DOC concentration peaks arrived 2 d earlier in coarse gravel and 5 d earlier in fine gravel at 500 m from the river axis (Figure 7, black triangles). The scenario in fine gravel with sand was not evaluated for DOC travel times because DOC concentration peaks never arrived at 500 m distance from the river axis during 60 d of simulation time. When DOC concentrations in the river additionally varied from 1 to 10 mg/l during the flood, simulated DOC concentration peaks arrived 14 d earlier in coarse gravel and 27 d earlier in fine gravel at the restored than at the steep riverbank at 500 m distance from the river (Figure 8, black triangles). The additional removal of a low hydraulic conductivity layer on top of the riverbank sediments after restoration caused that simulated DOC concentration peaks arrived 18 d earlier in coarse gravel and 27 d earlier in fine gravel at 500 m from the river axis (Figure 9, black triangles). Due to vertical gradients during the flood peak, vertical mixing caused that simulated DOC concentrations hit the bottom of the aquifer after 10 d (Figure 3, right). In case of clogging of the riverbank, the simulated DOC concentrations infiltrated preferably across the river bed causing vertical mixing below (Figure 6a). In reality, vertical mixing will depend on the effective vertical dispersivity, which is very much site-specific.

### *3.4. Comparative analysis*

When comparing the effects of riverbank topography, river concentration and hydraulic conductivity of the uppermost bank sediments, the topography was responsible for 51 % of the total increase in simulated DOC concentrations in coarse gravel, 84 % in fine gravel and 78 % in fine sandy gravel. The effect of the riverbank topography on DOC concentrations in groundwater was higher with an increase of DOC concentrations in the river during the flood than if they were assumed constant. The remainder is ascribed to the removal of a clogging layer on top of the riverbank sediments after restoration (49 % in coarse gravel, 16 % in fine gravel and 22 % in fine sandy gravel).

The surface topography of the riverbank was responsible for 77 % of the total earlier arrival times of simulated DOC concentration peaks at 500 m distance from the river axis in coarse gravel, and for 100 % in fine gravel. Again, the arrival times were by 12 to 22 d shorter when an increase in DOC concentrations of the river during the flood was assumed. The remainder can be ascribed to the removal of a clogging layer on top of the riverbank sediments after restoration (23 % in coarse gravel and 0 % in fine gravel).

## 4. Discussion

In Europe floodplains increasingly show signs of terrestrial ecosystems, following constructions of flood protection dikes and hydropower plants since the 19th century (Lair et al. 2009). This process led to an increased retention and demobilization of contaminants, which reach the river system via waste waters, surface water or atmospheric deposition and thus provide a sink for pollution, as found by Lair et al. 2009 for nitrate and phosphorous compounds. For the case of river floodplains, an increase in surface-groundwater exchange is most likely after restoration, leading to higher infiltration rates of contaminants into groundwater and potentially to their remobilization. Lair et al. (2009) suggested a way to overcome this problem was to conserve soil organic matter after restoration, facilitating degradation and thus the removal of DOC.

The aim of this paper was to comparatively quantify the effects responsible for enhancing DOC transport from the river into groundwater after riverbank restoration. Specifically, the effects on DOC concentration levels and DOC travel times towards distances from 400 to 500m from the river axis were investigated, where drinking water wells are commonly located.

### *4.1. Effects of riverbank restoration on groundwater DOC concentration*

First, the effects on DOC concentration levels are discussed. The simulated DOC concentration peaks were generally higher and arrived earlier for the restored than for the steep riverbank, with the largest differences after the largest flood assumed (5 m) and at closest distance to the river. Derx et al. (2010) and (2013a) made strong variations in pore velocities and river-aquifer mixing responsible for enhanced solute and virus transport from the river into groundwater. These mechanisms apply also in our simulations for DOC transport.

In a statistical cluster analysis of data from 33 riverbank filtration sites in various countries, Skark et al. (2006) identified the most important factors for DOC elimination being the initial DOC concentration in the river, the hydraulic conductivity (transmissivity) of the aquifer and the residence time in groundwater. In accordance with Skark et al. (2006), our simulations showed that the effect of changes in riverbank topography after restoration on enhancing DOC transport from the river into groundwater can be strongly amplified by increases in DOC concentrations in the river during floods and by changes in riverbank hydraulic conductivity. In previous studies, DOC concentrations in rivers were found to be related to river discharges e.g. in the Danube and Missouri rivers, with the same ranges of DOC concentrations and river discharge rates as in our simulations (Wolfram and Humpesch 2003, Raymond and Oh 2007). This emphasizes the importance for reducing contaminant levels in rivers, specifically if river floods occur on a regular basis. For example, similar sized flood events as assumed in our simulations occur at the river Danube on average once a year (via donau 1997). In such cases, where the submerged area of the riverbank during a flood is similarly large as in our simulations (i.e. 250 m in width or larger), near-river groundwater quality may therefore be at higher risk of being contaminated after restoration.

At restored riverbanks mass fluxes across the river-aquifer interface increase. Derx et al. (2010) e.g. observed that hydraulic pressure gradients changed from groundwater exfiltration to infiltration during floods at the river Danube. Our simulations further indicated that the removal of a clogging layer during bank restoration can further enhance DOC transport into groundwater, especially in coarse gravel. This process can lead to an increase in hydraulic conductivity of the uppermost sediments of the riverbank. The higher DOC concentration levels during the peak of the flood, however, are eventually compensated by more dilution after the flood due to return flows from groundwater towards the river. As a consequence for the scenarios at the restored riverbank, the return flows occurring after the peak of the floods led to a dilution effect in groundwater and below the river bed. This was because in the simulations, fresh water containing low concentrations of DOC was brought from inland. After a longer time period and numerous flooding events, however, a clogging layer may re-establish on top of the restored bank and this dilution effect may decrease.

Interestingly for the scenario at the steep riverbank, the return flows caused that DOC discharged from the groundwater below the river bed (Figures 3c and 6). Robinson et al. (2007) similarly observed a subterranean discharge of fresh groundwater, which they explained by tidal forcing, producing oscillating landward- and seaward- directed hydraulic gradients in the nearshore aquifer. While at the ocean, tides are oscillating on a daily basis, this effect also shows in our simulations at a river after one single flood event.

Unsaturated-saturated flow conditions were of minor importance in our simulations. A sensitivity analysis for virus transport from a river with first-order decay indicated that variations in water saturation and in the parameters for the unsaturated zone had small effects on the simulated concentrations (Derx et al. 2013a). Strong precipitation events or during inundation of overland areas may cause that unsaturated flow and transport from the top surface become more important. In this paper, however, we have not considered overland flows, as we focused on more frequent flooding events.

### 4.2. Effect of riverbank restoration on groundwater DOC travel times

Secondly, the effects of riverbank restoration on travel times of DOC from the river towards certain distances from the river are discussed. The simulations showed that at a restored riverbank, travel times of DOC concentration peaks towards distances from 400 to 500 m from the river axis can be reduced by 18 to 27 d compared with at steep riverbanks. Our simulations indicated that a change in surface topography of the riverbank, i.e. a larger submerged area during floods, can be very important for decreasing travel times of DOC concentration peaks from the river towards distances from 400 to 500 m from the river axis. In contrast to a commonly uniform surface topography of steep riverbanks, the surface topography at restored riverbanks can be rougher and more heterogeneous. Top surface heterogeneities may additionally enhance river-aquifer mixing and thus further enhance the transport into the near-river aquifer, as shown by Derx et al. (2010) for solutes. Vogt et al. (2010) studied the travel times of electric conductivity signals in an alluvial aquifer of the Thur River (Switzerland) after a similar sized flood event ($\Delta$h = 3 m) and similar aquifer properties as in our simulations. Indeed, they observed a longer travel time, but at a shorter distance from the river than in our simulations (at 50 m). A more heterogeneous riverbank topography such as at the River Thur is very likely to occur also at other rivers after restoration. This emphasizes that after the restoration of riverbanks, the risk of groundwater contamination may increase, potentially requiring additional treatment to achieve the required drinking water quality.

The simulations suggest that groundwater quality may be impaired after riverbank restoration, specifically after large flood events leading to significant soil erosion and to contaminated river water. The risk of contamination of drinking water wells near rivers may increase. These effects may not only apply for DOC but qualitatively also for other organic pollutants and microbial pathogens that occur in waters (e.g. viruses), and may have important implications for the water supply at restored bank sites. Such implications could be to prohibit river revitalization in the inner protection zone of drinking water wells, such as done in Switzerland (BUWAL 2004) or to develop further monitoring strategies. Future drinking water safety management has to consider such potential quality changes due to riverbank restoration and take appropriate measures (e.g. increased water treatment, large setback distances, advanced monitoring, etc..).

## 5. Conclusion

This paper is a comparative analysis of the effects caused by riverbank restoration on enhancing DOC transport from the river into groundwater. Simulations indicate that at a restored riverbank, DOC concentrations peaks after a 5 m river flood event can be 1.7 to 9 times higher and arrive 18 to 27 d earlier at 400 to 500 m distance from the river axis in coarse to fine sandy gravel than at a steep riverbank.

In our simulations, 51 to 84 % of the increase in DOC concentration levels and 77 to 100 % of the decrease in DOC travel times towards distances from 400 to 500 m from the river axis were due to the change in surface topography, i.e. a larger area of the riverbank which was gradually submerged during floods. The effect was higher if DOC concentrations at the river boundary were assumed to increase during the flood. The remaining part was caused by an increased riverbank hydraulic conductivity assumed at the restored riverbank. Our simulations show that return flows after the peak of the flood can eventually compensate the immediate rise in DOC concentration levels in the near-river aquifer by more dilution with groundwater from inland. In the case that riverbank restoration projects are planned, we recommend evaluating if further monitoring or treatment is needed for the protection of drinking water resources near rivers.

For predicting the effects of riverbank restoration on the groundwater quality for specific sites, we recommend accounting for the complex transient groundwater flow situation in the near-river aquifer during flooding events, as they may, besides heterogeneities of the surface topography, significantly increase the infiltration capacity of contaminants from the river into groundwater. In the future, the effects of riverbank restoration on DOC concentrations in groundwater will need to be further explored by empirical time series during flooding events. The effects of pH, organic matter composition, redox conditions and pore velocity will have to be included, as they have strong effects on the soil's degradation capacity.

## 6. Acknowledgments

This paper was supported by the Austrian Science Fund (FWF) as part of the DKplus (Vienna Doctoral Program on Water Resource Systems, project number W1219-N22) and the GWRS-Vienna in cooperation with Vienna Water as part of the ″(New)Danube - Untere Lobau Network Project ″ (Gewässervernetzung (Neue) Donau - Untere Lobau (Nationalpark Donau-Auen) funded by the Government of Austria (Federal Ministry of Agriculture, Forestry, Environment & Water Management), the Government of Vienna, and the European Agricultural Fund for Rural Development (project LE 07-13). This is a joint investigation of the Interuniversity Cooperation Centre for Water & Health (www.waterandhealth.at).

## 7. References

## References

Blaschke, A., Steiner, K.H., Schmalfuss, R., Gutknecht, D., Sengschmitt, D., 2003. Clogging processes in hyporheic interstices of an impounded river, the Danube at Vienna, Austria. International Review of Hydrobiology 88, 397–413.

Boggs, J., Beard, L., Waldrop, W., Stauffer, T., MacIntyre, W., Antworth, C., 1993. Transport of tritium and four organic compounds during a natural-gradient experiment (MADE-2). Technical Report EPRI-TR-101998. Palo Alto, CA.

BUWAL, 2004. Wegleitung Grundwasserschutz. Bundesamt für Umwelt, Wald und Landschaft, Bern.

Chen, X., 2000. Measurement of streambed hydraulic conductivity and its anisotropy. Environmental Geology 39, 1317–1324.

Cunningham, A., Characklis, W., Abedeen, F., Crawford, D., 1991. Influence of biofilm accumulation on porous media hydrodynamics. Environmental Science and Technology 25, 1305–1311.

de Marsily, G., 1986. Quantitative Hydrogeology. Academic Press, New York.

Derx, J., Blaschke, A.P., Blöschl, G., 2010. Three-dimensional flow patterns at the river-aquifer interface - a case study at the Danube. Advances in Water Resources 33, 1375–1387.

Derx, J., Blaschke, A.P., Farnleitner, A., Pang, L., Blöschl, G., Schijven, J., 2013a. Effects of fluctuations in river water level on virus removal by bank filtration and aquifer passage - a scenario analysis. Journal of Contaminant Hydrology 147, 34–44.

Derx, J., Farnleitner, A.H., Zessner, M., Pang, L., Schijven, J., Blaschke, A.P., 2013b. Evaluating the effect of temperature induced water viscosity and density fluctuations on virus and DOC removal during river bank filtration - a scenario analysis. River Systems 20, 169–184.

Fischer, T., Day, K., Grischek, T., 2005. Sustainability of riverbank filtration in Dresden, Germany, in: 5th International Symposium on Management of Aquifer Recharge, ISMAR, UNESCO, Berlin, Germany. pp. 23–28.

van Genuchten, M., 1980. A closed-form equation for predicting the hydraulic conductivity of unsaturated soils. Soil Science Society of America Journal 44, 892–898.

Grünheid, S., Amy, G., Jekel, M., 2005. Removal of bulk dissolved organic carbon (DOC) and trace organic compounds by bank filtration and artificial recharge. Water Research , 3219–28.

Grünheid, S., Jekel, M., 2005. Fate of bulk organics during bank filtration of wasterwater-impacted surface waters., in: 5th International Symposium on Management of Aquifer Recharge, ISMARS, UNESCO, Berlin, Germany. pp. 548–554.

Hickin, E.J., 1995. River Geomorphology. Wiley, Chichester.

Hoehn, E., 2002. Hydrogeological issues of riverbank filtration - a review., NATO Scientific Affairs Division. pp. 17–41.

Hoehn, E., Scholtis, A., 2011. Exchange between a river and groundwater, assessed with hydrochemical data. Hydrology and Earth System Sciences 15, 983–988.

Homonnay, Z., 2002. Use of bank filtration in Hungary, in: Ray, C. (Ed.), Riverbank filtration: understanding contaminant biogeochemistry and pathogen removal, NATO Scientific Affairs Division. pp. 17–41.

Hülshoff, I., Greskowiak, J., Wiese, B., Grützmacher, G., 2009. Relevance and opportunities of bank filtration to provide safe water for developing and newly industrialised countries, in: TECHNEAU 5.2.9 - Combination of MAR and adjusted conventional treatment processes for an Integrated Water Resources Management, European Commission.

Kinzelbach, W., 1987. Numerische Methoden zur Modellierung des Transports von Schadstoffen im Grundwasser. R. Oldenbourg Verlag München Wien.

Kirschner, A., Kavka, G., Velimirov, B., Mach, R., Sommer, R., Farnleitner, A., 2009. Microbiological water quality along a 2600 km longitudinal profile of the Danube river: Integrating data from two whole-river surveys and a transnational monitoring network. Water Research 43, 3673–3684.

Krüger, C., Radakovich, K., Sawyer, T., Barber, L., Smith, R., Field, J., 1998. Biodegradation of the surfactant linear alkylbenzenesulfonate in sewage-contaminated groundwater. A comparison of column experiments and field tracer tests. Environmental Science and Technology 32, 3954–3961.

Lair, G., Zehetner, F., Fiebig, M., Gerzabek, M., van Gestel, C., Hein, T., Hohensinner, S., Hsu, P., Jones, K., Jordan, G., Koelmans, A., Poot, A., Slijkerman, D., Totsche, K., Bondar-Kunze, E., Barth, J., 2009. How do long-term development and periodical changes of river-floodplain systems affect the fate of contaminants? results from european rivers. Environmental Pollution 157, 3336–3346.

Ludwig, U., Grischek, T., Nestler, W., Neumann, V., 1997. Behavior of different molecular-weight fractions of DOC of Elbe river water during riverbank infiltration. Acta Hydrochim.Hydrobiol. 25, 145–150.

Maeng, S., Sharma, S., Lekkerkerker-Teunissen, K., Amy, G., 2011. Occurence and fate of bulk organic matter and pharmaceutically active compounds in managed aquifer recharge: A review. Advances in Water Resources 45, 3015–3033.

Orlikowski, D., Hein, T. (Eds.), 2006. Analyse und Auswertung vorhandener Grundwasserdaten in der Unteren Lobau aus den Jahren 1992 - 2005 - Analysis of groundwater data in the Lower Lobau from 1992 - 2005, City of Vienna *MA45*, Department for Water Engineering.

Partinoudi, V., Collins, M., 2007. Assessing RBF reduction/removal mechanisms for microbial and organic DBP precursors. Journal AWWA 99, 61–71.

Rausch, R., Schäfer, W., Therrien, R., Wagner, C., 2005. Solute Transport Modelling. Science Publishers, Berlin Stuttgart.

Raymond, P.A., Oh, N.H., 2007. An empirical study of climatic controls on riverine C export from three major U.S. watersheds. Global Biogeochemical Cycles 21, 1–9.

Regli, C., 2007. Groundwater protection for water engineering measures near rivers. Gas Wasser Abwasser 87, 521–528.

Robinson, C., Li, L., Barry, D., 2007. Effect of tidal forcing on a subterranean estuary. Advances in Water Resources 30, 851–865.

Samaritani, E., Shrestha, J., Fournier, B., Frossard, E., Gillet, F., Guenat, C., Niklaus, P., Tockner, K., Mitchell, E., Luster, J., 2011. Heterogeneity of soil carbon pools and fluxes in a channelized and a restored floodplain section (Thur River, Switzerland). Hydrology and Earth System Sciences 15, 1059–1091.

Schaap, M.G., Leij, F.J., Van Genuchten, M.T., 2001. ROSETTA: A computer program for estimating soil hydraulic parameters with hierachical pedotransfer functions. Journal of Hydrology 251, 163–176.

Schmidt, C., Lange, F., Brauch, H.J., Kühn, W., 2003. Experiences with riverbank filtration and infiltration in Germany. Technical Report. DVGW-Water Technology Center (TZW). Karlsruhe, Germany.

Schönheinz, D., Grischek, T., 2011. Behaviour of dissolved organic carbon during bank filtration under extreme climate conditions, in: Ray, C., Shamrukh, M. (Eds.), Riverbank filtration for water security in desert countries, NATO Public Diplomacy Division. pp. 51–67.

Schubert, J., 2006. Significance of hydrologic aspects on RBF performance, in: Hubbs, S. (Ed.), Riverbank filtration hydrology, pp. 17–41.

Shankar, V., Eckert, P., Ojha, C., König, C., 2009. Transient three-dimensional modeling of riverbank filtration at Grind well field, Germany. Hydrogeology Journal 17, 321–326.

Shields, F., 1996. Hydraulic and hydrologic stability. Bookcraft (Bath) Ltd., Midsomer Norton, Somerset.

Skark, C., Remmler, F., Zullei-Seibert, N., 2006. Classification of riverbank filtration sites and removal capacity, in: Gimbel, R. (Ed.), Recent Progress in Slow Sand and Alternative Biofiltration Processes, IWA Publishing, London, UK.

U.S. Army Corps of Engineers, 2008. HEC-RAS - River analysis system. Technical Report. Davis, CA.

via donau, 1997. Die kennzeichnenden Wasserstände der österreichischen Donau (KWD 1996). Technical Report. Vienna, Austria.

Vogt, T., Hoehn, E., Schneider, P., Freund, A., Schirmer, M., Cirpka, O., 2010. Fluctuations of electric conductivity as a natural tracer for bank filtration. Advances in Water Resources 33, 1296–1308.

Voss, C.I., Provost, A.M., 2008. SUTRA - a model for saturated - unsaturated variable-density ground water flow with solute or energy transport. Technical Report Water-Resources Investigations Report 02-4231. Reston, Virginia.

Weiss, W., Bouwer, E., Aboytes, R., LeChevallier, M., O'Melia, C., Le, B., Schwab, K., 2005. Riverbank filtration for control of microorganisms: Results from field monitoring. Water Research 39, 1990–2001.

Weiss, W., Bouwer, E., Ball, W., O'Melia, C., LeChevallier, M., Arora, H., Speth, T., 2003. Riverbank filtration-Fates of DBP precursors and selected microorganisms. Journal of American Water Works Association 95, 68–81.

Wolfram, G., Humpesch, U. (Eds.), 2003. New Danube 2002: Effects of differently high water events on the New Danube., City of Vienna *MA45* and the Austrian Hydro Power AG (*Verbund*).

Woolsey, S., Capelli, F., Gonser, T., Hoehn, E., Hostmann, M., Junker, B., Paetzold, A., Roulier, C., Schweizer, S., Tiegs, S., Tockner, K., Weber, C., Peter, A., 2007. A strategy to assess river restoration success. Freshwater Biology 52, 752–769.

Figure 1: Cross section through the 3D water flow and transport model (Section 2.1); steep riverbank (top left) and restored site (bottom left). Map view of the model indicating area that is affected by riverbank restoration (brown shading, right). Vertical and horizontal discretizations of the numerical element mesh are depicted (top left and right)..

Figure 2: River water levels (left) and DOC concentrations (right) at the river boundary during steady flow simulations ($\Delta$h=0) and during increases of river water levels by 3 and 5 m.

Figure 3: Cross section W-E (see Figure 1) of DOC concentrations (colours) and groundwater flow directions (black arrows) for fine gravel, simulated with head changes in the river ($\Delta h$) of 0 m, (left) 3 m (centre) and 5 m (right); shown are DOC concentrations after 10 d (a and b) and after 30 d (c and d). Groundwater flow directions are shown after 20 d in rows c and d; DOC concentrations at the river boundary varied in time (Figure 2, right).

Figure 4: Peak DOC concentrations at the bottom of the groundwater aquifer at 60 d of simulation time; Blue and red lines correspond to non restored and restored situations; For the location of the zero point of the x-axis, see Figure 3. The scales of the axis are adjusted for improved visibility of the results.

Figure 5: As Figure 4, but with DOC concentrations at the river boundary varying in time (Figure 2, right).

Figure 6: As Figure 3, but simulated with a 30 cm clogging layer on top of the river bed and on top of the steep riverbank ($K_f = 10^{-6}$ m/s).

Figure 7: Simulated DOC concentrations in groundwater over time at the bottom of the groundwater aquifer at a restored and a steep riverbank; Red and blue lines correspond to restored and non restored situations; The black triangles refer to DOC concentration peaks during the simulation time; the scales of the axes are adjusted for improved visibility of the results.

Figure 8: As Figure 7, but with DOC concentrations at the river boundary varying in time (Figure 2, right).

Figure 9: As Figure 8, but simulated with a 30 cm clogging layer on top of the river bed and of the steep riverbank ($K_f = 10^{-6}$ m/s).

Table 1: Notation

| | |
|---|---|
| C | concentration of DOC (mg/l) |
| $D$ | 3-D dispersion tensor ($m^2/s$) |
| $\vec{g}$ | gravity vector ($ms^{-2}$) |
| h | aquifer depth (m) |
| $\Delta$h | total difference in river level (m) |
| $i$ | hydraulic groundwater gradient (m/km) |
| K | 3-D aquifer permeability matrix ($m^2$) |
| $K_f$ | hydraulic conductivity (m/s) |
| $\lambda$ | DOC decay rate of the adsorbable and biodegradable portion ($d^{-1}$) |
| p | hydraulic water pressure ($kN/m^2$) |
| $s_{op}$ | specific pressure storativity $(kg/ms^2)^{-1}$ |
| t | simulation time (d) |
| $\vec{v}$ | pore velocity (m/d) |
| $\alpha_l$ | longitudinal dispersivity (m) |
| $\alpha_t$ | transversal dispersivity (m) |
| $\vec{\nabla}$ | differential operator (-) |
| $\rho$ | fluid density (999.7 $kg/m^3$ at 10°C) |
| $\Theta$ | effective porosity (-) |
| $\Theta_w$ | water saturation (-) |
| $\mu$ | fluid viscosity ($1.307 \cdot 10^{-3}$ kg/ms at 10°C) |

**Figure**

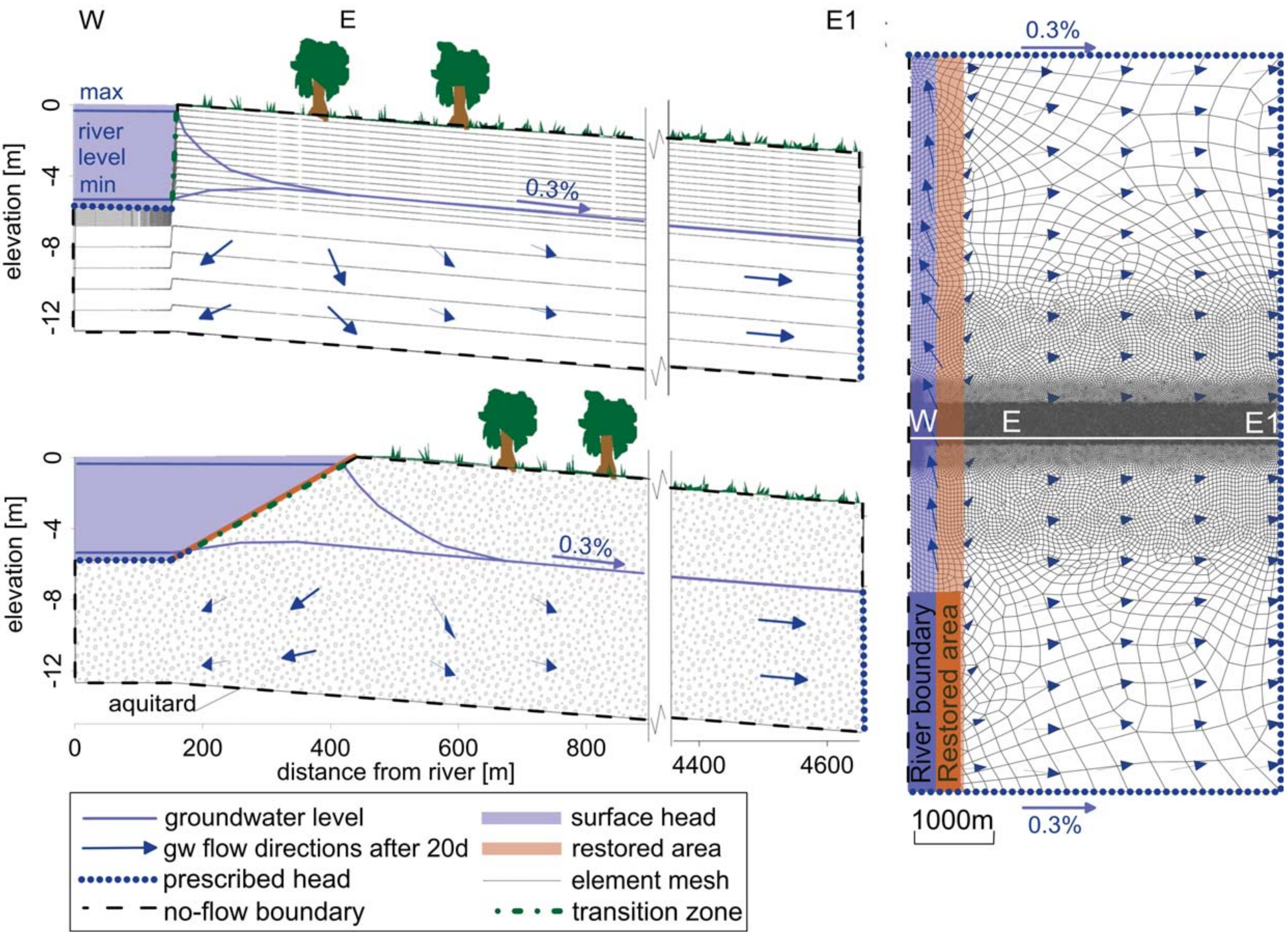

W
E
E1
max
river
level
min
0.3%
elevation [m]
0
-4
-8
-12
aquitard
0
200
400
600
800
4400
4600
distance from river [m]
groundwater level
gw flow directions after 20d
prescribed head
no-flow boundary
surface head
restored area
element mesh
transition zone
River boundary
Restored area
1000m

**Figure**

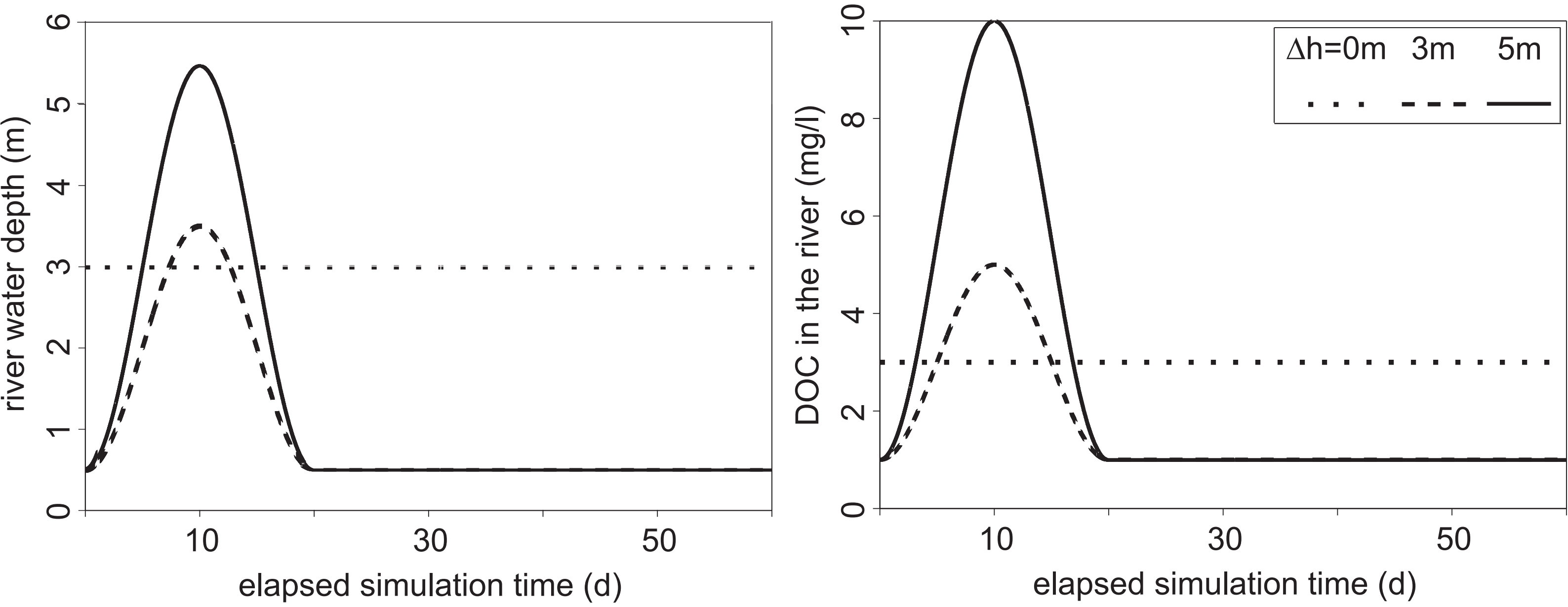

river water depth (m)
0
1
2
3
4
5
6
10
30
50
elapsed simulation time (d)
DOC in the river (mg/l)
0
2
4
6
8
10
Δh=0m 3m 5m
10
30
50
elapsed simulation time (d)

**Figure**

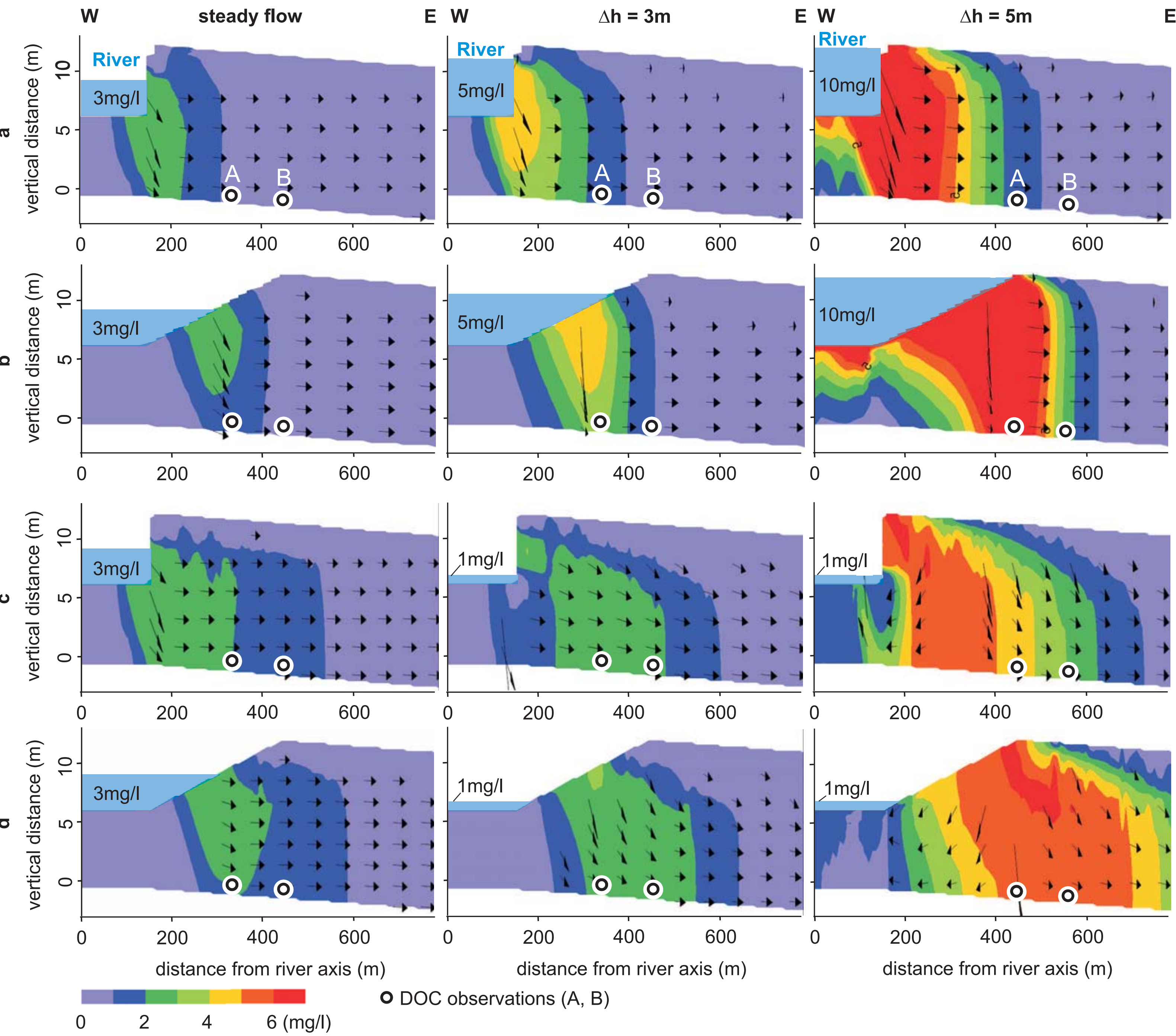

W
steady flow
E
W
Δh = 3m
E
W
Δh = 5m
E
River
3mg/l
River
5mg/l
River
10mg/l
A
B
a
b
c
d
vertical distance (m)
3mg/l
5mg/l
10mg/l
3mg/l
1mg/l
1mg/l
3mg/l
1mg/l
1mg/l
0
5
10
0
200
400
600
distance from river axis (m)
0
2
4
6 (mg/l)
DOC observations (A, B)

**Figure**

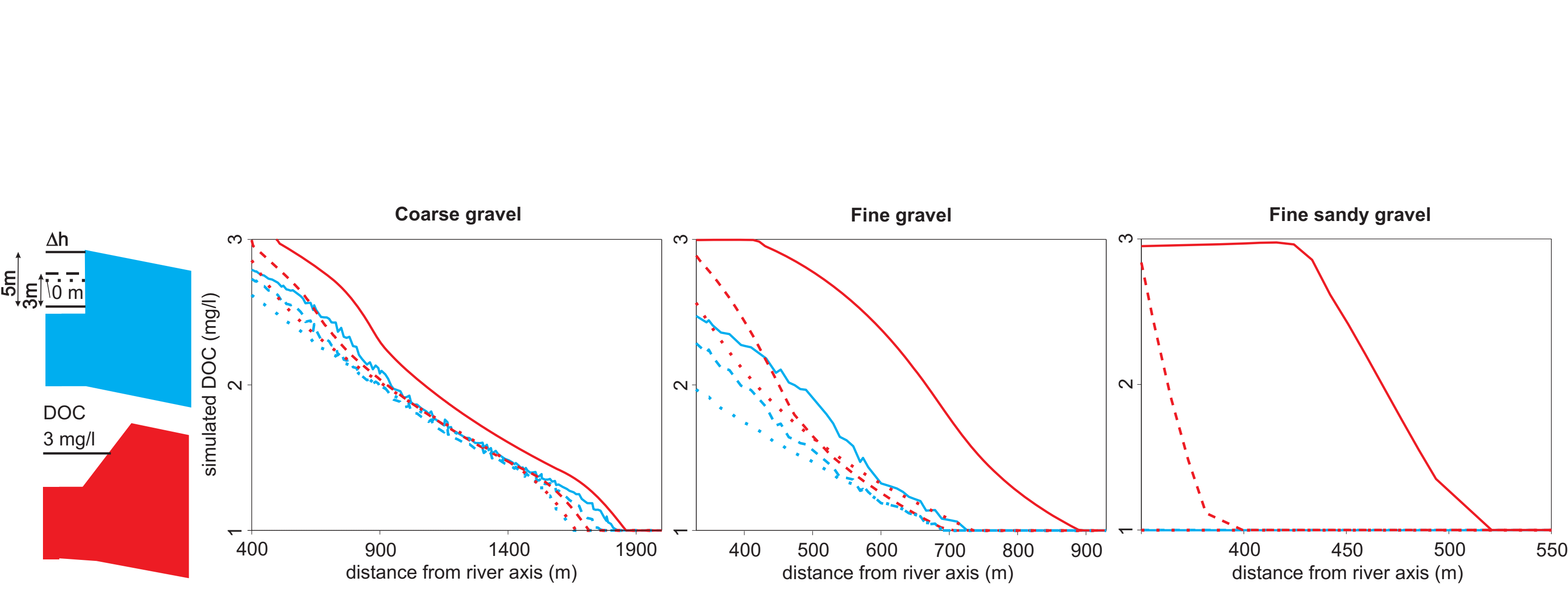

Δh
5m
3m
0 m
DOC
3 mg/l
Coarse gravel
Fine gravel
Fine sandy gravel
simulated DOC (mg/l)
3
2
1
400
900
1400
1900
500
600
700
800
450
550
distance from river axis (m)

**Figure**

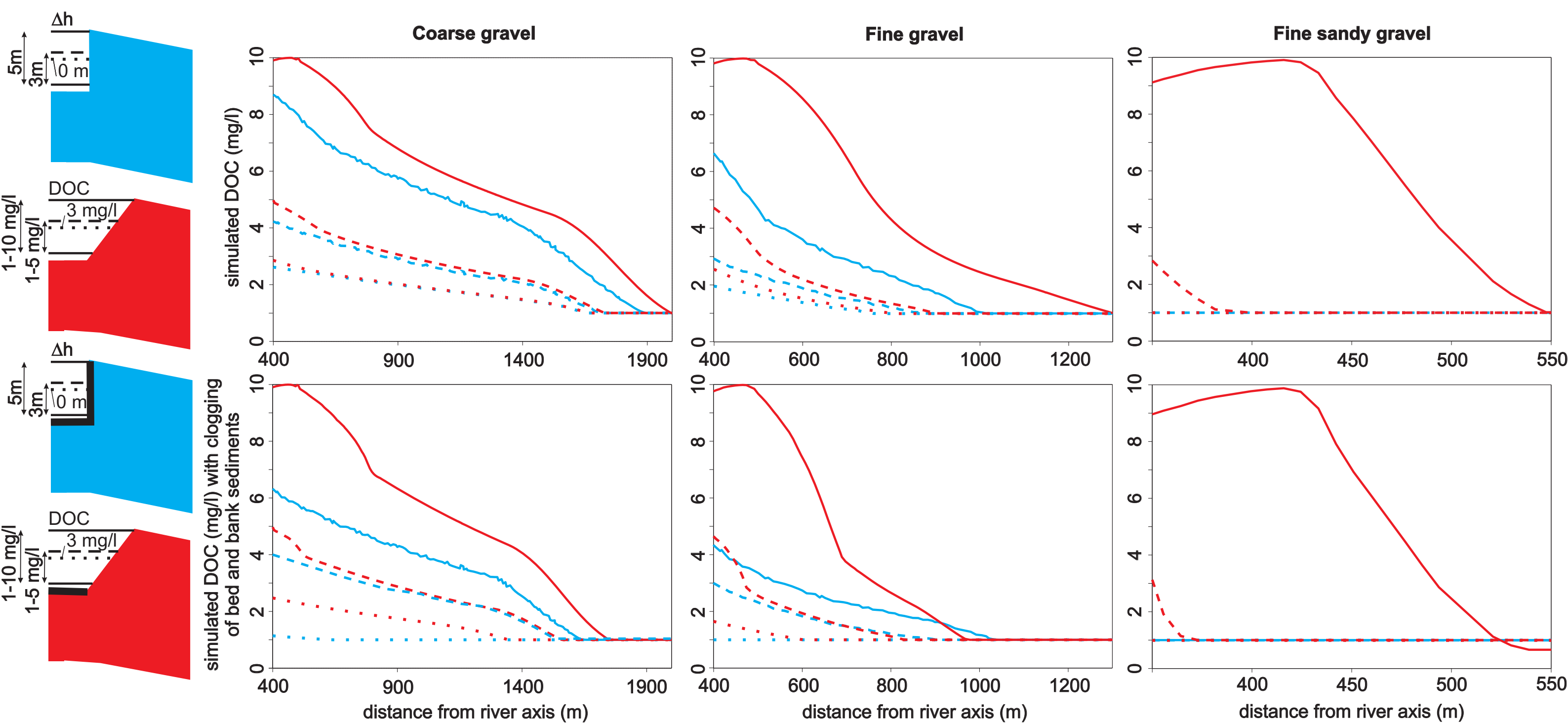

Δh
5m
3m
0 m
DOC
1-10 mg/l
1-5 mg/l
3 mg/l
Coarse gravel
Fine gravel
Fine sandy gravel
simulated DOC (mg/l)
simulated DOC (mg/l) with clogging of bed and bank sediments
distance from river axis (m)

Figure

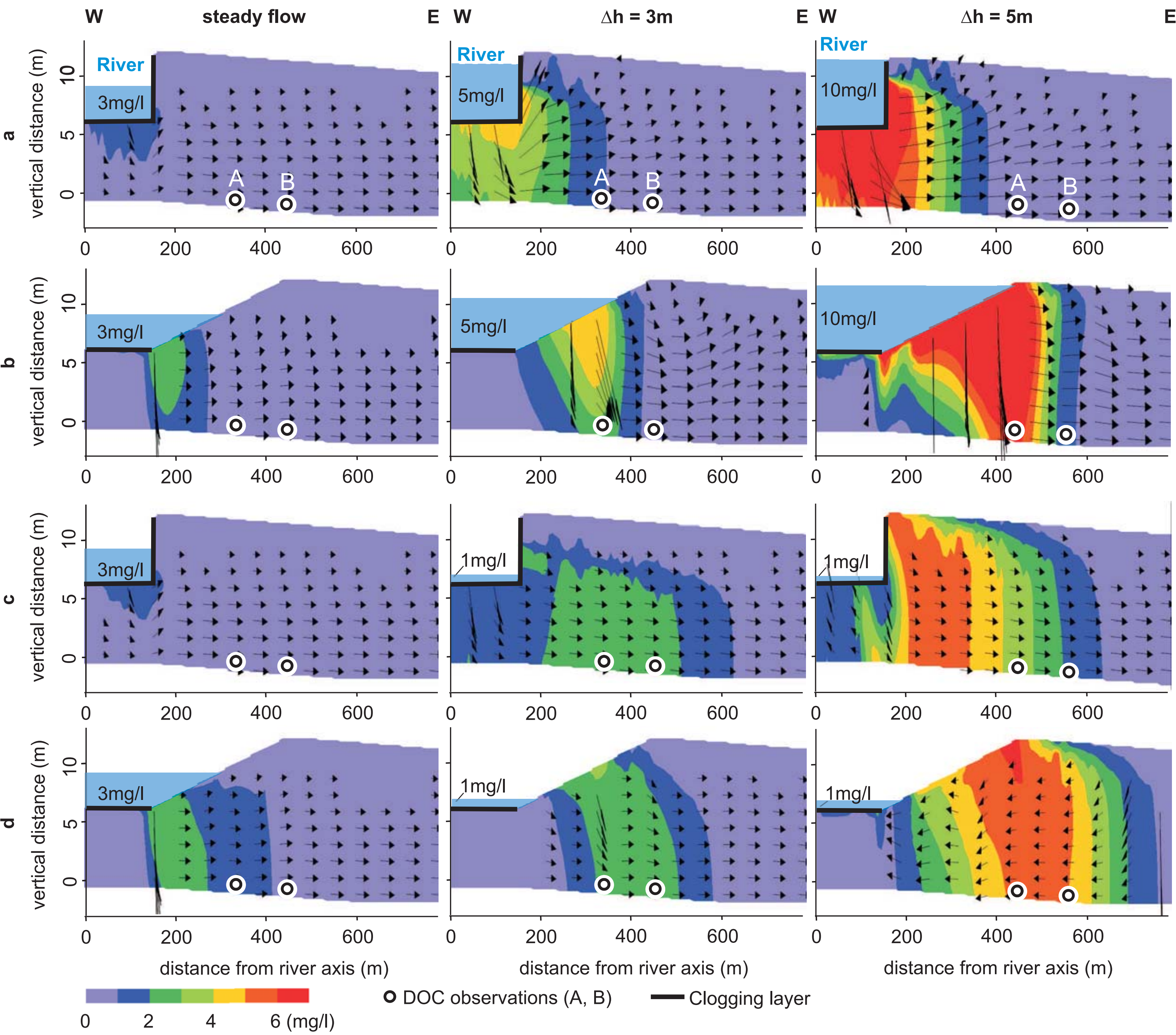
W
steady flow
E
W
Δh = 3m
E
W
Δh = 5m
E
a
b
c
d
River
3mg/l
5mg/l
10mg/l
1mg/l
A
B
vertical distance (m)
distance from river axis (m)
0
2
4
6 (mg/l)
DOC observations (A, B)
Clogging layer

**Figure**

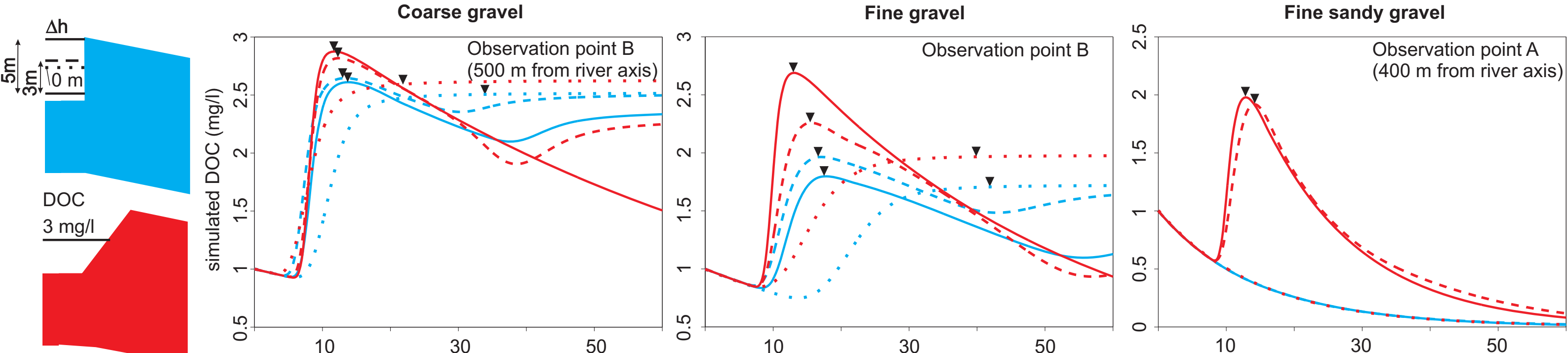

Δh
5m
3m
0 m
DOC
3 mg/l
Coarse gravel
Observation point B
(500 m from river axis)
simulated DOC (mg/l)
elapsed simulation time (d)
Fine gravel
Observation point B
elapsed simulation time (d)
Fine sandy gravel
Observation point A
(400 m from river axis)
elapsed simulation time (d)

Figure

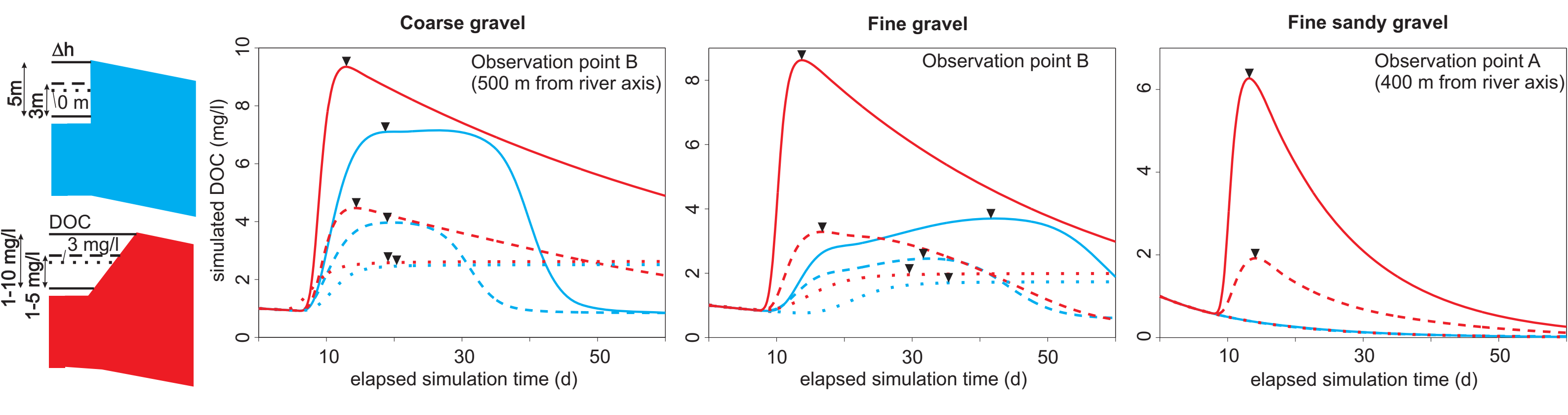

Δh
5m
3m
0 m
DOC
3 mg/l
1-10 mg/l
1-5 mg/l
Coarse gravel
Observation point B
(500 m from river axis)
simulated DOC (mg/l)
elapsed simulation time (d)
Fine gravel
Observation point B
elapsed simulation time (d)
Fine sandy gravel
Observation point A
(400 m from river axis)
elapsed simulation time (d)

Figure

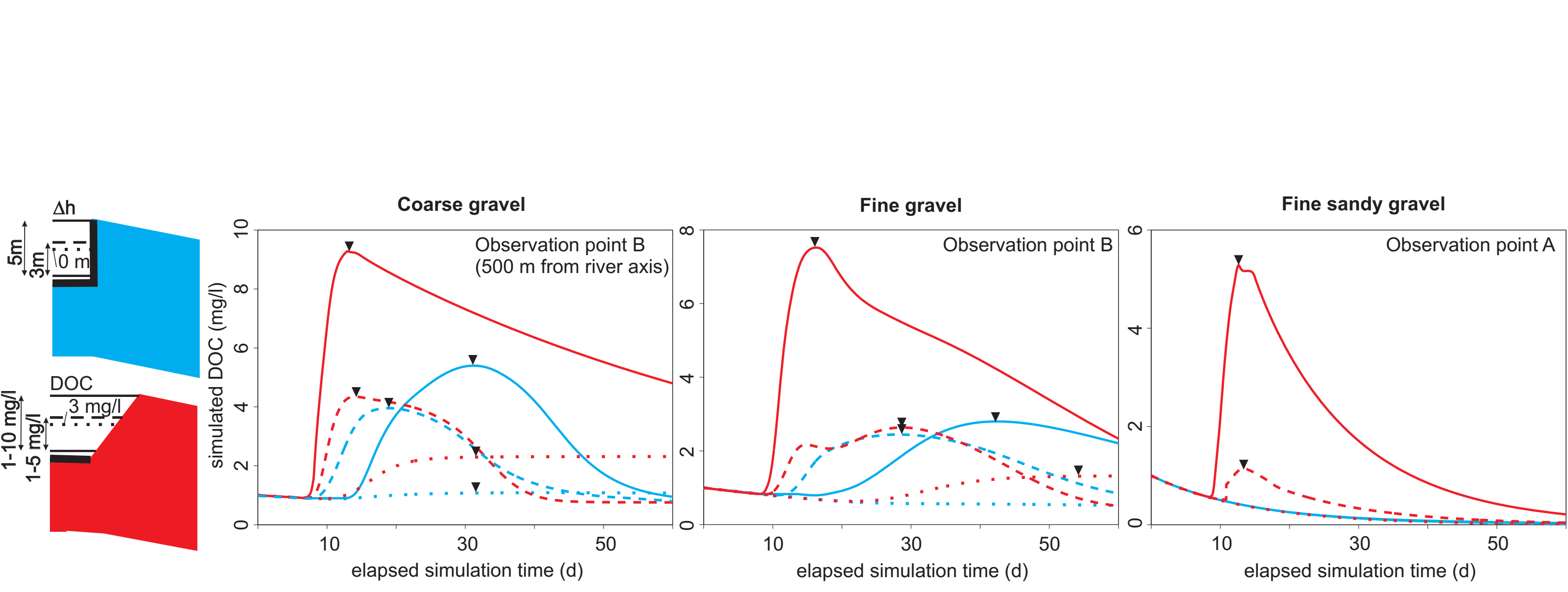

Δh
5m
3m
0 m
DOC
3 mg/l
1-10 mg/l
1-5 mg/l
Coarse gravel
Observation point B
(500 m from river axis)
Fine gravel
Observation point B
Fine sandy gravel
Observation point A
simulated DOC (mg/l)
elapsed simulation time (d)
elapsed simulation time (d)
elapsed simulation time (d)